Identification of bacterial determinants of tuberculosis infection and treatment outcomes: a phenogenomic analysis of clinical strains

Sydney Stanley, Caitlin N Spaulding, Qingyun Liu, Michael R Chase, Dang Thi Minh Ha, Phan Vuong Khac Thai, Nguyen Huu Lan, Do Dang Anh Thu, Nguyen Le Quang, Jessica Brown, Nathan D Hicks, Xin Wang, Maximillian Marin, Nicole C Howard, Andrew J Vickers, Wiktor M Karpinski, Michael C Chao, Maha R Farhat, Maxine Caws, Sarah J Dunstan, Nguyen Thuy Thuong Thuong, Sarah M Fortune

Summary

Background Bacterial diversity could contribute to the diversity of tuberculosis infection and treatment outcomes observed clinically, but the biological basis of this association is poorly understood. The aim of this study was to identify associations between phenogenomic variation in *Mycobacterium tuberculosis* and tuberculosis clinical features.

Methods We developed a high-throughput platform to define phenotype–genotype relationships in *M tuberculosis* clinical isolates, which we tested on a set of 158 drug-sensitive *M tuberculosis* strains sampled from a large tuberculosis clinical study in Ho Chi Minh City, Viet Nam. We tagged the strains with unique genetic barcodes in multiplicate, allowing us to pool the strains for in-vitro competitive fitness assays across 16 host-relevant antibiotic and metabolic conditions. Relative fitness was quantified by deep sequencing, enumerating output barcode read counts relative to input normalised values. We performed a genome-wide association study to identify phylogenetically linked and monogenic mutations associated with the in-vitro fitness phenotypes. These genetic determinants were further associated with relevant clinical outcomes (cavitary disease and treatment failure) by calculating odds ratios (ORs) with binomial logistic regressions. We also assessed the population-level transmission of strains associated with cavitary disease and treatment failure using terminal branch length analysis of the phylogenetic data.

Findings *M tuberculosis* clinical strains had diverse growth characteristics in host-like metabolic and drug conditions. These fitness phenotypes were highly heritable, and we identified monogenic and phylogenetically linked variants associated with the fitness phenotypes. These data enabled us to define two genetic features that were associated with clinical outcomes. First, mutations in *Rv1339*, a phosphodiesterase, which were associated with slow growth in glycerol, were further associated with treatment failure (OR 5·34, 95% CI 1·21–23·58, p=0·027). Second, we identified a phenotypically distinct slow-growing subclade of lineage 1 strains (L1.1.1.1) that was associated with cavitary disease (OR 2·49, 1·11–5·59, p=0·027) and treatment failure (OR 4·76, 1·53–14·78, p=0·0069), and which had shorter terminal branch lengths on the phylogenetic tree, suggesting increased transmission.

Interpretation Slow growth under various antibiotic and metabolic conditions served as in-vitro intermediate phenotypes underlying the association between *M tuberculosis* monogenic and phylogenetically linked mutations and outcomes such as cavitary disease, treatment failure, and transmission potential. These data suggest that *M tuberculosis* growth regulation is an adaptive advantage for bacterial success in human populations, at least in some circumstances. These data further suggest markers for the underlying bacterial processes that contribute to these clinical outcomes.

Funding National Health and Medical Research Council/A*STAR, National Institutes of Allergy and Infectious Diseases, National Institute of Child Health and Human Development, and the Wellcome Trust Fellowship in Public Health and Tropical Medicine.

Introduction

The determinants of tuberculosis treatment success, disease outcomes, and transmission involve a combination of host, environmental, and pathogen factors.[1,2] Outside of high-level drug resistance, we have a relatively superficial understanding of the *Mycobacterium tuberculosis* determinants of tuberculosis clinical outcomes, although the characterisation of bacterial determinants of relevant phenotypes could translate to clinical applications.[3]

Decades of work have identified *M tuberculosis* determinants of evolved drug resistance, including recent studies that have used *M tuberculosis* whole-genome sequencing (WGS) to

Lancet Microbe 2024

Published Online https://doi.org/10.1016/S2666-5247(24)00022-3

Department of Immunology and Infectious Diseases, Harvard T H Chan School of Public Health, Boston, MA, USA (S Stanley PhD, C N Spaulding PhD, Q Liu PhD, M R Chase PhD, J Brown MS, N D Hicks PhD, X Wang PhD, N C Howard PhD, A J Vickers BS, W M Karpinski BS, M C Chao PhD, Prof S M Fortune MD); **Pham Ngoc Thach Hospital, Ho Chi Minh City, Viet Nam** (D T M Ha MD PhD, P V K Thai MD PhD, N H Lan MD PhD); **Oxford University Clinical Research Unit, Hospital for Tropical Diseases, Ho Chi Minh City, Viet Nam** (D D A Thu BS, N L Quang MS, N T T Thuong PhD); **Department of Biomedical Informatics, Harvard Medical School, Boston, MA, USA** (M Marin PhD, M R Farhat PhD); **Department of Systems Biology, Harvard Medical School, Boston, MA, USA** (M Marin); **Pulmonary and Critical Care Medicine, Massachusetts General Hospital, Boston, MA, USA** (M R Farhat); **Liverpool School of Tropical Medicine, Liverpool, UK** (M Caws PhD); **Birat Nepal Medical Trust, Kathmandu, Nepal** (M Caws); **Department of Infectious Diseases, University of Melbourne at the Peter Doherty Institute for Infection and Immunity, Parkville, VIC, Australia** (S J Dunstan PhD); **Nuffield Department of Medicine, Centre for Tropical Medicine and Global Health, University of Oxford, Oxford, UK** (N T T Thuong); **Ragon Institute of MGH, MIT, and Harvard, Cambridge, MA, USA** (Prof S M Fortune); **Broad Institute of MIT and Harvard, Cambridge, MA, USA** (Prof S M Fortune)

Correspondence to:
Prof Sarah M Fortune,
Department of Immunology and Infectious Diseases, Harvard T H Chan School of Public Health, Boston, MA 02215, USA
sfortune@hsph.harvard.edu

Research in context

Evidence before this study

We used different combinations of the words "mycobacterium tuberculosis", "tuberculosis", "clinical strains", "intermediate phenotypes", "genetic barcoding", "phenogenomics", "cavitary disease", "treatment failure", and "transmission" to search the PubMed database for all studies published up until Jan 20, 2022. We only considered English language publications, which biases our search. Previous work has identified associations between *M tuberculosis* bacterial lineage, or less frequently, genetic polymorphisms and either phenotypic variation in experimental models of pathogenesis or clinical outcomes such as cavitary disease, treatment failure, delayed culture conversion, and transmission. Many of these studies focused on *M tuberculosis* strains from the global pandemic lineages 2 and 4. Several *M tuberculosis* genome-wide association studies had identified genetic associations with in-vitro drug resistance. Published laboratory-based studies of *M tuberculosis* clinical strains involved relatively small numbers of strains, did not identify the genetic basis of relevant phenotypes, did not experimentally test predicted phenotypes of the clinical strains, or did not link findings to the corresponding clinical outcomes. Two recent studies described phenogenomic analyses in *Mycobacterium abscessus* and *Plasmodium falciparum*.

Added value of this study

We developed a functional genomics platform to perform high-throughput phenotyping of *M tuberculosis* clinical strains. We then used these phenotypes as intermediate traits to identify novel bacterial genetic features associated with clinical outcomes. We found that mutations in *Rv1339*, an atypical phosphodiesterase, were associated with slow growth in glycerol and with treatment failure in patients. We also identified a subclade of *M tuberculosis* strains, characterised by slow growth in vitro under several metabolic conditions including media containing acetate plus propionate, and exposure to second-line drugs such as bedaquiline and clozafamine. This subclade was associated with cavitary disease, treatment failure, and increased transmission potential in Viet Nam.

Implications of all the available evidence

The bacterial intermediate phenotypes we identified might be directly related to the mechanisms of the adverse clinical outcomes, or they might serve as markers for the causal yet unidentified bacterial determinants. Via the intermediate phenotyping, we also discovered a surprising diversity in *M tuberculosis* responses to the new anti-mycobacterial drugs that target central metabolic processes, which will be important in considering roll-out of these new drugs. Our study and others that have identified *M tuberculosis* determinants of tuberculosis clinical and epidemiological phenotypes should inform efforts to augment diagnostics and drug regimen design, which might improve treatment outcomes and mitigate drug resistance and transmission.

find novel genetic determinants of drug susceptibility in *M tuberculosis*.[4] A few studies have sought to use similar approaches to find bacterial determinants of more complex clinical phenotypes, such as treatment relapse or failure, transmission, and dissemination.[5–10] However, these efforts have been limited by a paucity of well phenotyped tuberculosis cohorts, *M tuberculosis* genetic linkage resulting in covariance of spurious variants with causal mutations, and uncertainty about *M tuberculosis* pathobiology in patients.

See Online for appendix 1

The gap between bacterial genetics and complex clinical phenotypes is not unique to tuberculosis, as the mechanistic study of many human diseases faces similar challenges. As a potential solution, human geneticists turned to intermediate trait analysis to dissect the genetic determinants of disease and their mechanistic contributions.[11] Intermediate phenotypes are heritable biological traits shaped by the same genetic drivers as the more complicated disease processes under investigation, but they might be related to the clinical phenotype of interest in non-intuitive ways and they do not always establish causality. However, they can provide a genetic handle for, and mechanistic insights into, otherwise intractably complex clinical states. In this study, we developed a high-throughput phenogenomic platform for the discovery of intermediate traits intrinsic to *M tuberculosis* of two related clinical phenotypes: treatment failure and cavitary disease.[2]

Methods

Study design, participants, and *M tuberculosis* clinical isolates

We sought to develop a platform to identify *M tuberculosis* traits associated with infection and treatment outcomes (appendix 1 p 1). We used this approach to perform a secondary analysis of a subset (n=200) of 1635 *M tuberculosis* strains collected from a study of tuberculosis treatment outcomes in Ho Chi Minh City, Viet Nam (henceforth referred to as the primary study).[9] The primary study was performed between Dec 15, 2008, and June 20, 2011.[9] Patients presenting to any one of eight district tuberculosis units (DTUs) or the outpatient department of Pham Ngoc Thach Hospital were invited to participate. Patients included had pulmonary tuberculosis confirmed by sputum smear microscopy, were HIV-negative, and provided written informed consent. Patients who withheld or were unable to consent, had previously received tuberculosis treatment, had an HIV infection, were pregnant, were younger than 18 years, or were receiving treatment outside the DTUs were excluded. Lung cavitation was identified via chest radiography.[8] Treatment outcome was assessed within the Viet Nam national tuberculosis programme framework, which included evaluation of sputum smear at 2, 5, and 8 months, and on completion of treatment.[9] Treatment failure was defined as a positive sputum smear test at

5 months or 8 months (or both) and culture-positivity at 8 months. The primary study was approved by the institutional research board of Pham Ngoc Thach Hospital, Ho Chi Minh City, Viet Nam, and the Oxford University Tropical Research Ethics Committee (OxTREC 030–07); secondary analysis of the strains was deemed to not be human-subjects research by the Harvard Longwood Campus Institutional Review Board (IRB17-1576).

In this study, we analysed clinical strains that were found to be phenotypically drug sensitive to ethambutol, isoniazid, rifampicin, and streptomycin in the primary study (BACTEC MGIT 960 SIRE system, BD, Franklin Lakes, NJ, USA); pyrazinamide sensitivity testing was not standardised with this method at the time of the study and thus was excluded.[9] Before barcoding, phenotypic susceptibility to rifampicin was reconfirmed (appendix 2 p 2).

Barcoded *M tuberculosis* clinical strain library

For bacterial intermediate trait analysis, we selected a subset of 200 strains that were representative of the *M tuberculosis* lineage distribution of the entire cohort. Each clinical isolate, plus the reference strain, *M tuberculosis* Erdman, was transformed with an integrating plasmid library carrying a randomised 18 base pair DNA sequence tag. We aimed for three independent barcoded clones per strain to serve as biological replicates. We successfully barcoded 158 of 200 clinical strains; attrition occurred due to various factors including failed strain recovery after transport, inability to confirm phenotypic drug sensitivity, and dropout in the barcoding process. Due to technical dropout, 29 strains were represented by only a single clone and the remainder (n=129) were represented by two or three clones. In total, the library contained 355 unique barcodes. The barcoded strains were pooled together in roughly equal concentrations to form the input library, which we confirmed had balanced representation of each barcode by sequencing (appendix 2 pp 2, 8–9).

In-vitro competition experiments and data analysis

We passaged the library in triplicate in standard 7H9 media and 7H9 plus DMSO (MilliporeSigma, Burlington, MA, USA); defined carbon source media including acetate, dextrose, glycerol, propionate, lactate, acetate plus propionate, and dextrose plus glycerol (MilliporeSigma); 7H9 containing first-line antibiotics ethambutol, isoniazid, rifampicin, and streptomycin (MilliporeSigma); and 7H9 with second-line antibiotics bedaquiline (BioVision, Milpitas, CA, USA), clofazimine (MilliporeSigma), and pretomanid (MilliporeSigma). Carbon sources were added to concentrations of 0·1–0·2% w/v (appendix 2 p 2). Antibiotics were used at roughly the minimum inhibitory concentration (MIC) that inhibits growth of 50% of tested clinical isolates.[12–15] Conditions were designed to replicate metabolic stress during infection and probe an array of essential bacterial processes.[16] We measured the optical density of the cultures at days 3 and 6 after inoculation of the cultures with the input library to track bulk library growth (appendix 2 p 10). Genomic DNA was extracted from the input library and the cultures at days 3 and 6. We used deep sequencing to quantify barcode abundance, which we normalised for sequencing library depth and abundance in the input library (appendix 2 pp 2–3, 8). We evaluated technical reproducibility by comparing the same barcode across technical replicates with a principal component analysis (PCA) and biological reproducibility via Pearson correlations comparing the same strain independently tagged with multiple barcodes (appendix 2 p 3). To obtain the final relative fitness values, we averaged input normalised barcode read counts across the technical and biological replicates, and we determined the $\log_2$ fold change and coefficient of variation (appendix 2 p 3, appendix 3 pp 1–5, appendix 4 p 1). Relative fitness values are independent of barcode abundance in the input, and relative fitness from the stress conditions are largely independent of relative fitness in 7H9 (appendix 2 pp 11–12). We performed hierarchical clustering and a Spearman correlation analysis of the conditions based on strain day 6 relative fitness values (appendix 2 p 3).

See Online for appendix 3
See Online for appendix 4
See Online for appendix 2

Competition experiments were repeated for a subset of conditions to further assess the reproducibility (appendix 4 p 2). Single-strain growth curves and MIC assays were performed to validate the relative fitness values using strains that were among the most fit and least fit across representative conditions tested (appendix 1 p 2, appendix 2 p 4).

Genomic, phylogenetic, and mutation analyses

We repeated WGS of the 158 barcoded strains (200 Mbp Illumina DNA sequencing, SeqCenter, Pittsburgh, PA, USA; accession number PRJNA950969) to ensure the strains we phenotyped were paired to the sequences determined previously (accession number PRJNA355614) and for variant calling, lineage typing, and genetic antimicrobial resistance typing as described (appendix 2 pp 3–4).[7] We found discordance between our WGS and the original sequences for 18 strains and used the corrected sequences for our analyses (appendix 1 p 1).

To identify *M tuberculosis* variants associated with the relative fitness phenotypes, we used the Python (version 3.8.5) package Pyseer (version 1.3.10) to perform a bacterial genome-wide association study (GWAS).[17] We used the linear mixed model option and included only non-synonymous single-nucleotide polymorphisms (SNPs) and intergenic region mutations. We controlled for population structure with SNP-based similarity and distance matrices and by inputting the lineage assignment for each strain (appendix 2 p 4). As an additional control, we completed a GWAS on 7H9-normalised relative fitness values (appendix 2 p 3, appendix 4 p 3). Pyseer was also used to determine the heritability of the relative fitness phenotypes.

Assessment of *Rv1339* genetic variants

On the basis of our observation that *Rv1339* variants were associated with slow growth in glycerol and treatment outcome (see Results), to confirm the barcode-based

phenotyping and assess whether the GWAS variants shared a loss-of-function (LOF) phenotype, we completed single-strain growth curves in glycerol media using a clinical isolate carrying a *Rv1339* frameshift mutation and its closest genetic neighbour for comparison (appendix 1 p 2). In addition, since heterologous expression of *M tuberculosis Rv1339* in *Mycobacterium smegmatis* has been shown to alter adenosine triphosphate (ATP) flux,[18] we transformed *M smegmatis* MC^2155 with episomal plasmids expressing *M tuberculosis Rv1339* wild-type (WT) or GWAS variants and used the CellTiter-Glo Luminescent Cell Viability Assay (Promega, Madison, WI, USA) to measure the ATP levels according to the manufacturer's protocol (appendix 2 pp 4–5).[19] We also mined a database of published genome-wide LOF screens in *M tuberculosis* to identify conditions that favour *Rv1339* LOF.[20]

L1.1.1.1 subclade population genetics

As we also observed that L1.1.1.1 subclade clinical isolates were associated with cavitary disease and treatment failure (see Results), we used variant calling to identify mutations unique to L1.1.1.1 relative to the rest of the cohort to understand the genetic basis of the intermediate traits that characterise this subgroup (appendix 2 pp 3–4). We performed a bioinformatic functional annotation of biological processes impacted by the non-synonymous plus insertion or deletion mutations in L1.1.1.1 using The Database for Annotation, Visualization and Integrated Discovery (DAVID) webserver.[21] To examine the transmission dynamics of L1.1.1.1 and three other closely related L1 clades, we did a phylogenetic reconstruction of the 344 L1 strain WGS from the primary study and compared the terminal branch lengths of the subgroups according to published methodology (appendix 1 p 3, appendix 2 p 4).[5,7] We also used all 952 clinical isolates from a published dataset that reflects the global diversity of L1.1.1 and its subgroups to complete a phylogenetic comparison with the L1.1.1.1 strains in our cohort (appendix 1 p 4, appendix 2 p 4).[5,22]

Statistical analysis

We used the following statistical approaches to evaluate the major outcomes of this study: Kruskal–Wallis test for the assessment of relative fitness and intermediate traits across different conditions; Pyseer GWAS and Mann–Whitney test for the determination of the genetic basis and heritability of intermediate traits; odds ratio (OR) calculation by exponentiating the coefficients from binomial logistic regressions tests for the association of clinical outcomes with the genetic determinants of intermediate phenotypes; unpaired *t* test for the phenotypic validation of a GWAS link between a monogenic variant and an intermediate phenotype associated with treatment failure; and Kruskal-Wallis test for the terminal branch length analysis of a subclade of *M tuberculosis* strains associated with cavitary disease and treatment failure. We also used ORs to evaluate the association between patient age, sex, or infecting *M tuberculosis* lineage with clinical outcomes; we completed both single variable and multivariable associations adjusted with all factors.

We utilised the stats package (version 4.3) of R (version 4.2.2) for PCA, Pearson correlations, and OR analyses. Mann–Whitney, Kruskal–Wallis, ANOVA, Spearman correlations, and unpaired *t* tests were performed with Prism 9 (version 9.5.0). In all cases, we set a significance threshold of 0·05.

Role of the funding source

The funders of the study had no role in study design, data collection, data analysis, data interpretation, or writing of the report.

Results

To identify bacterial determinants of clinical phenotypes in our subset of 158 *M tuberculosis* strains, we first took a canonical approach and evaluated associations of *M tuberculosis* lineage with treatment outcomes. In our cohort, 42 (27%) of 158 strains were lineage 1 (L1), 107 (68%) were lineage 2 (L2), and nine (6%) were lineage 4 (L4; figure 1A, appendix 1 p 1). Among the 158 patients whose strains were represented in this cohort, cavitary disease occurred in 44 (28%) patients and treatment failure in 14 (9%) patients. Infection with an L1 strain, but not with an L2 or L4 strain, was significantly associated with treatment failure (OR 3·96, 95% CI 1·29–12·82, p=0·017); lineage was not associated with cavitary disease (table). 114 (72%) of the 158 strains were from male patients, 44 (28%) were from female patients, and the median age of the patients was 40 years (IQR 28·75–47·25); these features were not associated with the clinical outcomes (table).

As *M tuberculosis* lineage is a coarse discriminator that provides relatively little information as to the contributing biological processes, we developed a competitive fitness platform for the high-throughput profiling of *M tuberculosis* strains to define intermediate traits that might elucidate relevant biological features and their underlying genetic determinants (appendix 2 p 8). We found sound technical reproducibility in our relative fitness measurements as indicated by PCA (appendix 2 p 13) and sound biological reproducibility; the median Pearson correlation coefficient for the fitness of independently tagged isolates of the same strain across all conditions was 0·91 (IQR 0·76–0·97) while the correlation coefficient for different strains was –0·04 (IQR –0·32 to 0·30; Mann-Whitney p<0·0001, appendix 2 p 13). The relative fitness for each strain in each condition is shown in appendix 3 p 4. The Spearman correlation coefficients of the relative fitness values from fully independent repeats of the competition experiments ranged from 0·72 to 0·97 (appendix 2 p 14).

The strains displayed a broad range of fitness phenotypes across the metabolic and antibiotic conditions tested, with the distributions of strain abundance varying over time such that by day 6, the median relative fitness values across conditions were significantly different from each other (Kruskal-Wallis p<0·0001; figure 1B). Therefore,

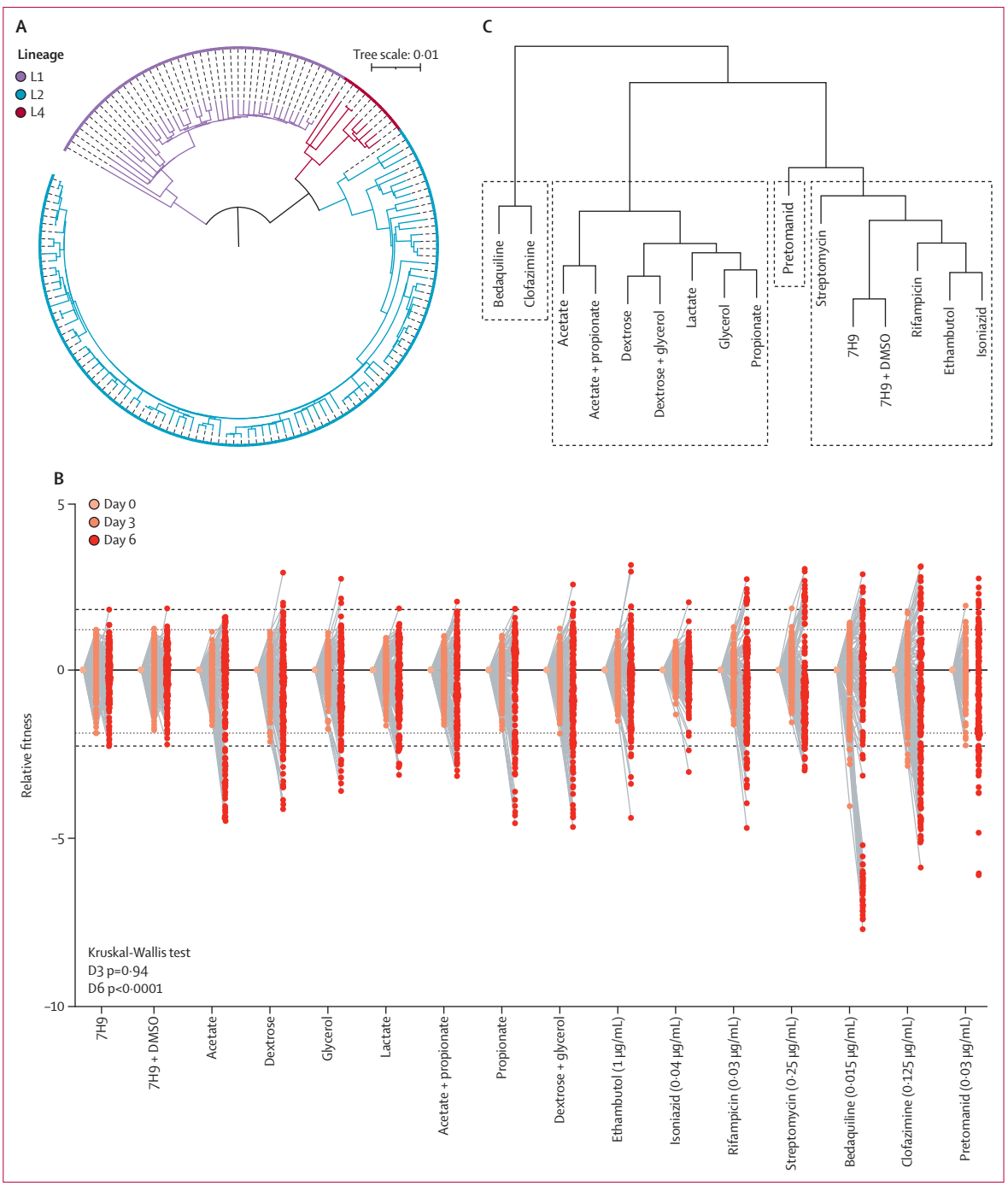

***Figure 1: Mycobacterium tuberculosis* clinical isolates genetically barcoded for pooled competition experiments to examine relative metabolic and antibiotic fitness phenotypes**
(A) Approximate maximum-likelihood tree of the 158 *M tuberculosis* strains selected for the study and the reference strain, *M tuberculosis* Erdman. The scale indicates the number of mutations per site; the tree is rooted at the midpoint. (B) Dot plot of relative fitness values for all 159 strains per indicated condition and timepoint. All carbon sources were added to concentrations of 0·1–0·2% w/v. Relative fitness values were normalised to strain abundance in input pool inoculum, so all day 0 values are set to zero. Kruskal-Wallis comparison of the distribution of relative fitness values across conditions for each timepoint is shown. (C) Ward's linkage clustering of the stress conditions based on strain day 6 relative fitness values, with agglomerative coefficient=0·76. Boxes denote four different k-mean clusters. DMSO=dimethylsulfoxide.

subsequent analyses were done with day 6 values. Relative fitness values from similar carbon source conditions (such as acetate and acetate plus propionate) and drugs with related mechanisms of action (ethambutol and isoniazid or bedaquiline and clofazimine) were highly correlated (figure 1C, appendix 2 p 13). The relative fitness values from carbon source conditions formed a distinct cluster from the antibiotic conditions (figure 1C). We validated relative

	Cavitary disease				Treatment failure			
	OR (95% CI)	p value	Adjusted OR (95% CI)	Adjusted p value	OR (95% CI)	p value	Adjusted OR (95% CI)	Adjusted p value
Age, years	1·015 (0·99–1·043)	0·29	1·013 (0·99–1·042)	0·36	1·017 (0·97–1·06)	0·42	1·011 (0·99–1·055)	0·60
Sex								
Female	0·96 (0·43–2·06)	0·92	1·17 (0·51–2·64)	0·70	0·69 (0·15–2·33)	0·58	1·079 (0·22–4·15)	0·92
Male	1 (ref)	..	1 (ref)	..	1 (ref)	..	1 (ref)	..
Infecting strain lineage								
L1	1·92 (0·89–4·11)	0·095	1·87 (0·85–4·10)	0·12	3·96 (1·29–12·82)	0·017	3·84 (1·21–12·84)	0·023
L2	1 (ref)	..	1 (ref)	..	1 (ref)	..	1 (ref)	..
L4	0·89 (0·13–3·96)	0·89	0·80 (0·11–3·65)	0·79	NA	NA	NA	NA

Data are odds ratio (95% CI), unless otherwise stated. 1 (ref) denotes the reference level for each variable, which was selected based on the number of observations. There were no instances of treatment failure in patients infected by an L4 strain, so this variable was excluded from analyses of treatment failure associations; this is indicated by NA.

Table: **Clinical outcomes associated with culture-confirmed tuberculosis disease from a sample of 158 patients from Viet Nam**

See Online for appendix 5

fitness values determined by our competitive fitness assay with traditional single-strain growth assays. MIC assays of bedaquiline, clofazimine, pretomanid, and streptomycin confirmed that strains with the highest relative fitness values have MICs as much as 15 times greater than that of strains with the lowest relative fitness values, although all were still under critical concentrations defining high-level drug resistance (appendix 2 p 15).[23] Single-strain growth curves in acetate plus propionate defined media also confirmed that strains with the largest relative fitness values grew faster than the strains with the lowest relative fitness values (appendix 2 p 16).

To assess the genetic basis of the relative fitness phenotypes, we calculated the heritability of each phenotype, which estimates the amount of variation in a phenotype that can be explained by genetic variation. The pretomanid phenotype had the lowest heritability (0·46), whereas the heritability of most other phenotypes was greater than 0·75 (appendix 2 p 17), suggesting strong genetic contribution to these phenotypes. Given these data and the association between infection with L1 *M tuberculosis* and treatment failure in our cohort, we compared the intermediate phenotypes of each lineage. The relative fitness values were significantly lower for L1 than for L2 and L4 across nearly every condition, but especially in acetate, acetate plus propionate, bedaquiline, and clofazimine (figure 2). A notable exception was pretomanid, where L1 strains were relatively more fit than L2 and L4 strains (figure 2). Moreover, even within a lineage, the distribution of relative fitness values was clearly bimodal in some conditions, such as bedaquiline for L1, suggestive of bacterial determinants of relative fitness beyond lineage.

See Online for appendix 6

We sought to explicitly define genetic determinants of the intermediate phenotypes using a GWAS linear mixed model approach that allowed us to use the intermediate traits as continuous variables.[17] We mapped the GWAS hits onto the phylogenetic tree to identify residual population effects not corrected for in the linear mixed model approach (figure 3A). Associations with relative fitness under several carbon and antibiotic stress conditions were dominated by mutations shared by the L1.1.1.1 subclade of L1 (figure 3A, appendix 2 p 17, and appendix 5).[22] Indeed, in nine of 16 conditions, L1.1.1.1 strains drove the differences seen for L1 versus L2 and L4 strains (appendix 2 p 18). The GWAS also identified five monogenetic associations unlinked to L1.1.1.1. These were variants in *Rv1339*, a phosphodiesterase,[18] associated with lower relative fitness in glycerol ($p=6{\cdot}0\times10^{-6}$); *nuoD*, a subunit of the NADH dehydrogenase, linked to lower relative fitness in acetate plus propionate ($p=4{\cdot}6\times10^{-6}$); *Rv1687c*, an ATP-binding protein in an ABC transporter, linked to lower relative fitness in acetate plus propionate ($p=4{\cdot}3\times10^{-6}$); *Rv1707*, a putative sulfate permease linked to antibiotic persistence, associated with increased relative fitness in the presence of rifampicin ($p=4{\cdot}6\times10^{-6}$);[24] and *Rv3230c*, a NADPH oxidoreductase,[25] associated with decreased fitness in acetate plus propionate ($p=1{\cdot}4\times10^{-5}$; appendix 2 p 17, appendix 5 p 1). GWAS with 7H9-normalised relative fitness values yielded results consistent with those found with input-normalised relative fitness values, but interestingly allowed us to identify associations of variants in *Rv0409* with decreased relative fitness in the presence of ethambutol ($p=1{\cdot}29\times10^{-6}$), which is consistent with the fact that a whole-genome knockdown screen to identify genes that control the potency of antimycobacterial drugs has identified a significant association between *Rv0409* knockdown and sensitivity to ethambutol (appendix 2 p 19, appendix 6).[26]

We next asked whether infection with *M tuberculosis* strains carrying any of these genetic variants was associated with poor clinical outcomes. Infection with *M tuberculosis* strains carrying *Rv1339* variants was significantly associated with treatment failure (OR 5·34, 95% CI 1·21–23·58; p=0·027; figure 3B). Infection with L1.1.1.1 strains was associated with treatment failure (OR 4·76, 1·53–14·78; p=0·0069) and cavitary disease (2·49, 1·11–5·59; p=0·027; figure 3B), despite no previous association between cavitary disease and the L1 lineage (table). These associations were not confounded by patient age or sex (appendix 1 p 5). There were no associations with clinical outcomes for variants in *nuoD*, *Rv1687c*, *Rv1707*, *Rv3230c* (figure 3B), or *Rv0409* (appendix 6 p 1).

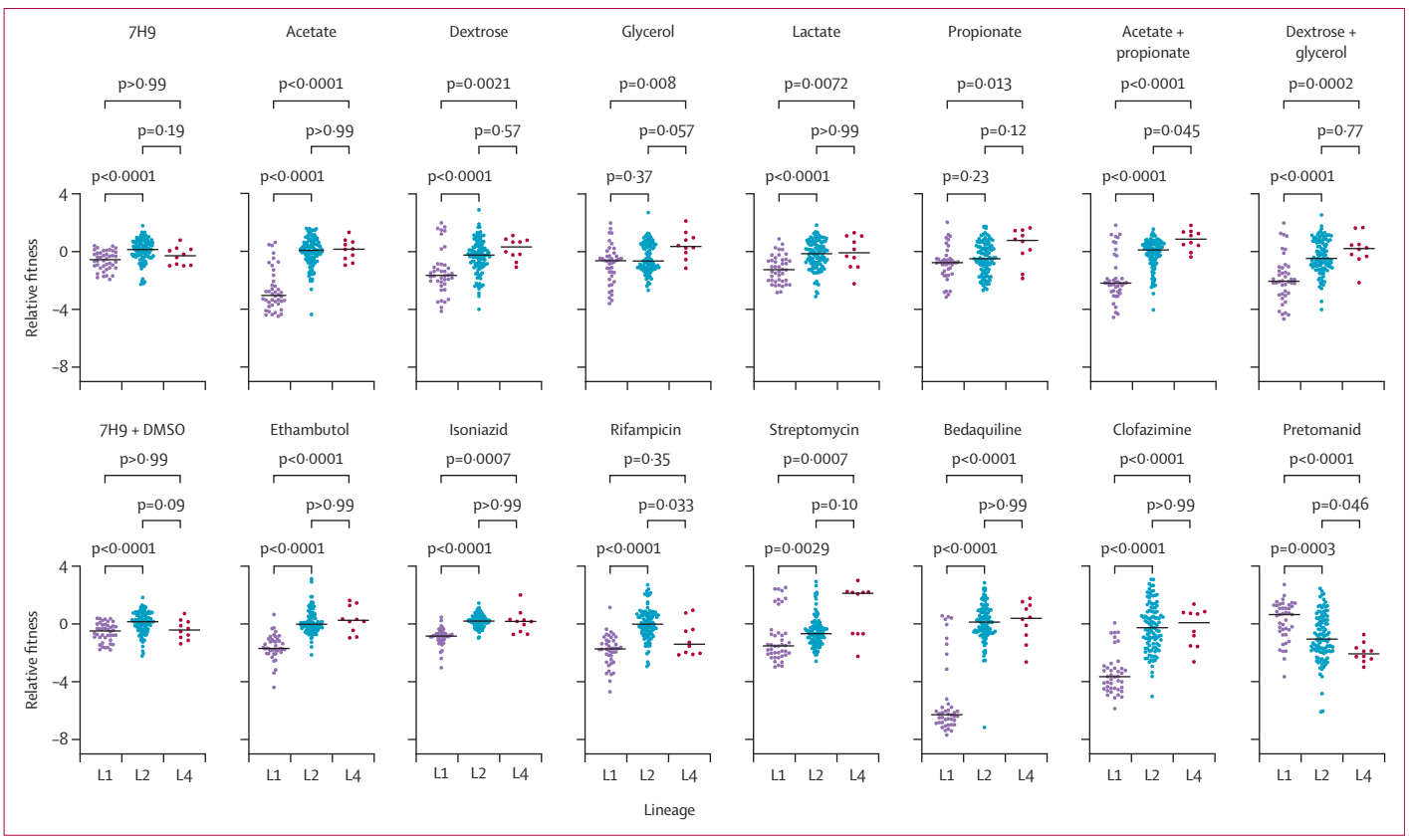

Figure 2: **Lineage patterns of antibiotic and metabolic relative fitness phenotypes of *Mycobacterium tuberculosis* clinical isolates**
Dot plot of strain relative fitness values for the indicated conditions, grouped by lineage. Horizontal lines denote medians. Kruskal-Wallis p values adjusted by the Dunn's multiple comparisons test indicated.

A clinical strain containing an *Rv1339* codon 217 frameshift mutation had lower relative fitness in glycerol than did its closest genetic relative, a phenotype which we confirmed with single-strain growth curves (appendix 1 p 2, appendix 2 p 20). The glycerol phenotype of the *Rv1339* frameshift variant resembled other *Rv1339* variants in the strain set, suggesting that the *Rv1339* GWAS SNPs are LOF (appendix 2 p 20). *Rv1339* modulates bacterial ATP flux;[18] and the expression of the catalytically dead $Rv1339^{Asp180Ala}$ variant in *M smegmatis*, along with the expression of GWAS variants $Rv1339^{Leu23Phe}$, $Rv1339^{Gly87Glu}$, and $Rv1339^{Gly164Val}$ resulted in higher ATP concentrations than those from expression of $Rv1339^{WT}$ and $Rv1339^{Arg19Arg}$ (figure 4A), further suggesting that the GWAS variants result in some degree of LOF. According to source data from published *M tuberculosis* genome-wide LOF screens, disruptions in *Rv1339* are neutral under many conditions but have very strong fitness advantages in host-relevant conditions such as in-vitro hypoxia and in mice that model human obesity and type 2 diabetes (NZO.H1Ltj; figure 4B).[27,28]

Understanding the physiology of phylogenetically linked phenotypes is more complicated than monogenic traits. A comparative genomics analysis revealed that the L1.1.1.1 strains in our cohort shared 103 private mutations (appendix 1 p 6). These included a premature stop codon in *mmpL5*, a gene encoding an efflux pump associated with bedaquiline and clofazimine resistance, which might explain the GWAS link between L1.1.1.1 and bedaquiline susceptibility ($p=1{\cdot}3\times10^{-6}$) and also L1.1.1.1 decreased fitness in clofazimine (figure 3A; appendix 2 pp 17–18).[26,29] Despite no GWAS association with pretomanid, the L1.1.1.1 strains in our cohort share a non-synonymous mutation in the pretomanid resistance determinant *fgd1*.[29] A functional annotation analysis indicated that L1.1.1.1 private mutations are involved in fatty acid degradation (p=0·0054), fatty acid metabolism (p=0·0068), and biosynthesis of cofactors (p=0·045; appendix 1 pp 6–7), consistent with the GWAS association with decreased fitness in acetate plus propionate ($p=6{\cdot}0\times10^{-6}$; appendix 2 pp 17–18).

Given these genetic differences, we compared the epidemiological fitness of L1.1.1.1 to other L1 clades using terminal branch lengths as a proxy for the maximum evolutionary time after transmission.[7] The terminal branch lengths of L1.1.1.1 strains were significantly smaller than those of the other L1 strains in the primary study, which might be indicative of a more recent transmission (figure 4C; appendix 2 p 21). We then compared the L1.1.1.1 strains in our sample with 952 L1.1.1.1 and L1.1.1 strains from a globally representative dataset.[5,22] The L1.1.1.1 strains used in our analysis did not form a distinct

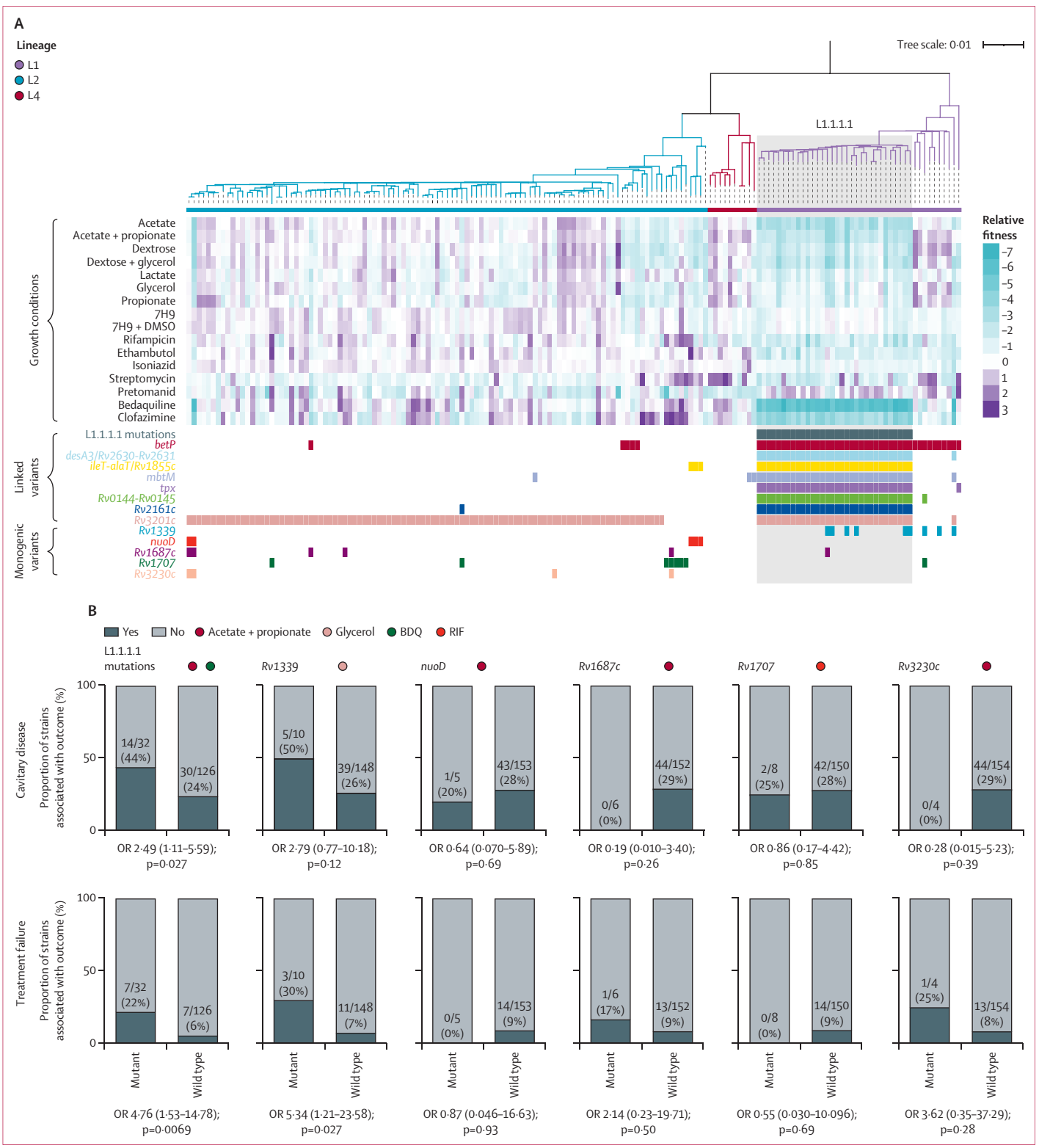

***Figure 3*: Identification of genetic determinants associated with intermediate phenotypes and poor tuberculosis treatment outcomes with a GWAS**

(A) Heatmap of strain day 6 relative fitness values ordered according to the phylogeny shown in figure 1. Colour squares mark strains carrying mutations in the indicated genes returned as significant hits from the GWAS after multiple test correction; reported mutations have an allele frequency of >2%. Conditions are ordered according to the hierarchal clustering from figure 1C. (B) Percentage and fraction of strains associated with the indicated clinical outcomes, grouped by genotype for the indicated genes. Coloured dots indicate the associated intermediate phenotype as determined by the GWAS. Data from input-normalised relative fitness values are shown in (A) and (B). GWAS=genome-wide association study. OR=odds ratio.

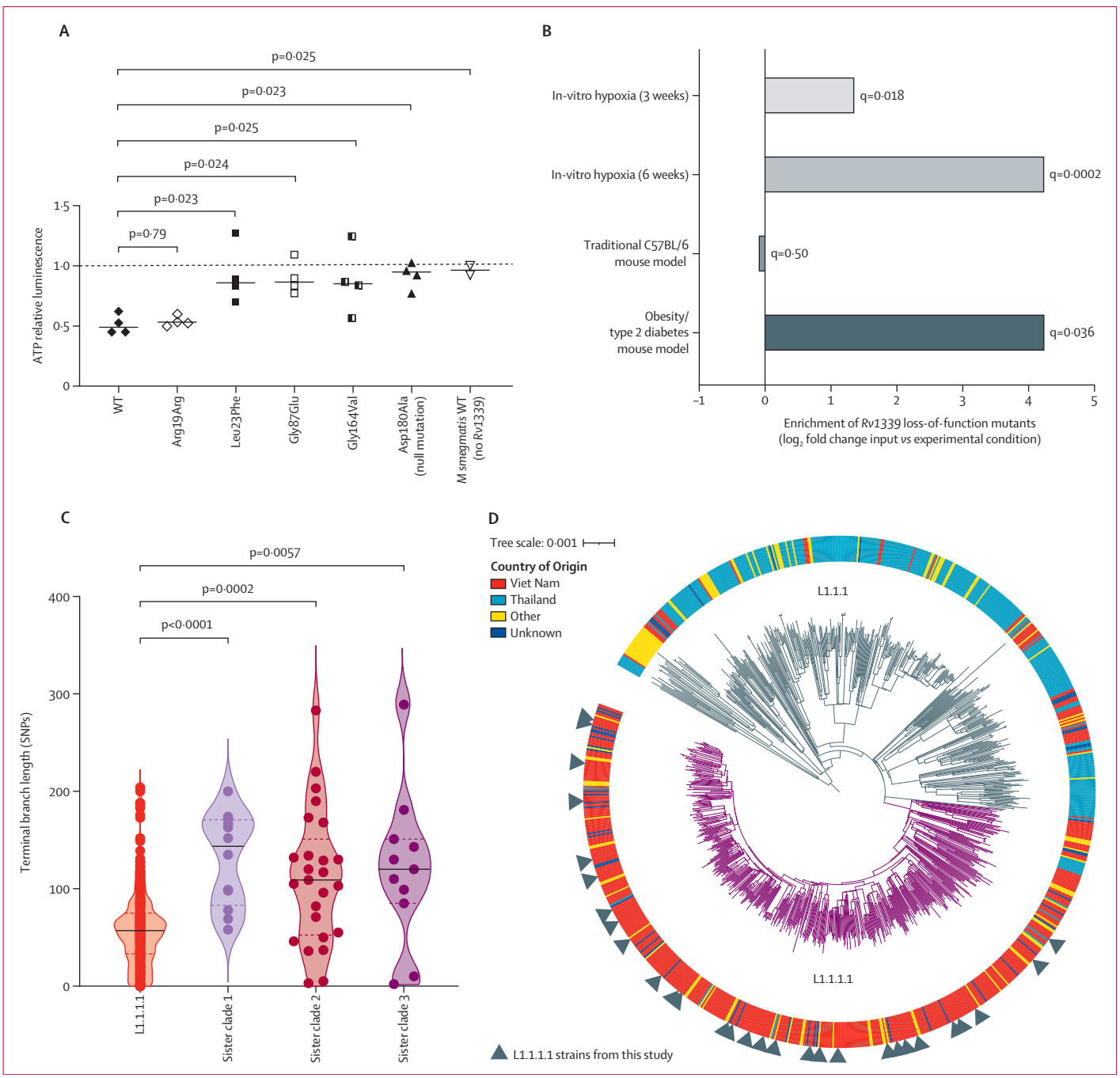

Figure 4: **Link between phenogenotypes of *Mycobacterium tuberculosis* associated with poor tuberculosis outcomes and in-vivo fitness and transmission**
(A) ATP concentrations in recombinant *Mycobacterium smegmatis* strains expressing the indicated *M tuberculosis Rv1339* genotype. The solid line denotes the mean and the p values denote the results of an unpaired *t* test. Each point represents the mean of technical replicates for an independent experiment. (B) Review of published genome-wide LOF screens using the *M tuberculosis* reference strain H37Rv.[20,27,28] Fold change refers to the representation of *Rv1339* LOF mutants in the input inoculum compared with the abundance in the indicated condition. q values indicate p values adjusted for multiple testing correction. (C) Violin plots of terminal branch lengths determined by SNPs for different clades of L1. p values from Kruskal-Wallis test and Dunn's multiple comparison test in comparison to L1.1.1.1 are indicated. Black line denotes the median. (D) Phylogenetic tree of 952 clinical isolates representing the global diversity of L1.1.1.1 and L1.1.1 *M tuberculosis* clinical strains. LOF=loss-of-function. SNP=single-nucleotide polymorphism. WT=wild type.

monophyletic group within the larger L1.1.1.1 clade but were instead interspersed throughout (figure 4D). This finding suggests that the L1.1.1.1 intermediate phenotypes we describe are representative of the entire clade. Consistent with previous observations, we found that, of the strains sampled across the world, 417 (79%) of the 527 L1.1.1.1 strains originated in Viet Nam, while 295 (69%) of the 425 L1.1.1 strains were isolated in Thailand.[7,30] Therefore, these

related clades demonstrate remarkable restriction within two distinct but proximal geographic regions, which mirrors the phenotypic distinction between L1.1.1.1 and the remainder of L1 strains (appendix 2 p 18).

Discussion

High-throughput phenotyping of *M tuberculosis* clinical isolates revealed unexpected diversification of bacterial metabolic preferences, which in some cases correlates with clinical outcomes. Here, we found that mutations associated with lower relative fitness under in-vitro conditions were associated with worsened clinical outcomes, which might seem counter-intuitive. However, *M tuberculosis* is a slow-growing organism and fully arrests growth in environmental conditions that simulate the granuloma, such as hypoxia, which is thought to be important for persistence in the face of drug treatment.[31] Indeed, we have previously described clinically prevalent variants in *prpR* that cause conditional slow growth in propionate and lead to multidrug tolerance.[4] Thus, the growth slowing that we observed could be an intermediate bacterial trait directly related to growth arrest in-vivo and a direct contributor to clinical outcomes. Alternatively, decreased fitness in certain metabolic conditions might be secondary to the processes directly driving clinical outcomes.

Here, we found both monogenic (*Rv1339*) and phylogenetically linked variants (L1.1.1.1 subclade) that were associated with worse infection outcomes. We previously found that *Rv1339* variants frequently emerged within patients, providing orthologous support for the association of *Rv1339* mutations with treatment failure.[5] It is possible that for both *Rv1339* variants and L1.1.1.1, host factors interact with the bacterial variants to shape outcome. It is striking that L1.1.1.1 is highly transmissible and prevalent in Viet Nam but rare in Thailand, despite geographic proximity.[7,30] This finding might suggest that *M tuberculosis* is following population-specific evolutionary trajectories. Future work should assess if different sub-lineages or monogenic variants associate with poor clinical outcomes in other biogeographic contexts. However, the slow growth intermediate phenotypes that we defined could be broadly relevant across different regions. In addition, terminal branch length analyses might be shaped by extenuating factors beyond transmission such as bacterial mutation rate and sample size; additional analyses must be used to assess L1.1.1.1 transmission dynamics more definitively.

The L1.1.1.1 subgroup also carries clade-defining mutations in genes known to modulate resistance to not only bedaquiline but also clofazimine and pretomanid, even though these drugs are not yet part of the standard antitubercular regimen.[32] These data are consistent with other reports of subclade-defining mutations in *mmpL5* and *fgd1*.[33,34] *M tuberculosis* strains might have evolved mutations—probably in response to host pressure on bacterial energy metabolism or small molecule transport—that ultimately alter sensitivity to these new antibiotics. These genomic changes in genes linked to altered bedaquiline, clofazimine, and pretomanid sensitivity should be considered both to limit the emergence of additional drug resistance and potentially in tailoring tuberculosis treatment to maximise efficacy.[35]

Together, our work highlights the utility of conducting high-throughput phenotyping of clinical strains to define intermediate fitness phenotypes linking negative clinical outcomes to genomic mutations of interest. These phenogenomic features might prove useful as both tools for dissecting mechanisms of *M tuberculosis* pathogenesis and clinically relevant biomarkers associated with treatment failure and cavitary disease.

Contributors

SS, CNS, QL, NTTT, and SMF were responsible for conceptualisation of the study. SS, CNS, MRC, JB, NDH, XW, and SMF contributed to methodology design. MC, SJD, NTTT, and SMF contributed to project administration. SS, QL, MRC, and NDH contributed to software development. SS, QL, MRC, MM, and MCC did the formal analyses. SS, CNS, DTMH, PVKT, NHL, DDAT, NLQ, JB, NDH, NCH, AJV, and WMK contributed to the experimental investigation. NTTT and SMF provided resources. SS wrote the original draft. SS, QL, MCC, and SMF contributed to the writing, review, and editing of the manuscript. SS and QL contributed to the visualisation of the data. MRF, MC, SJD, NTTT, and SMF supervised the study. SJD, NTTT, and SMF contributed to funding acquisition. All authors had full access to all the data in the study and accept responsibility for the decision to submit for publication. SS, QL, and SMF verified the underlying data of the study.

Declaration of interests

We declare no competing interests.

Data sharing

All whole-genome sequencing data from the study are available through the National Center for Biotechnology Information Sequence Read Archive via the project accession number PRJNA950969. The accession numbers for individual strains are available in appendix 1 (p 1).

Acknowledgments

This study was funded by the National Institutes of Allergy and Infectious Diseases (P01AI132130 [SS, SMF]; P01AI143575 [XW, SMF]; U19AI142793 [QL, SMF]; 5T32AI132120-03 [SS]; 5T32AI132120-04 [SS]; 5T32AI049928-17 [SS, SMF]; T32GM135014 [SMF]); the National Institute of Child Health and Human Development (5T32HD040128-19 [SS]); the Wellcome Trust Fellowship in Public Health and Tropical Medicine (097124/Z/11/Z [NTTT]); and the National Health and Medical Research Council/A*STAR joint call (APP1056689 [SJD]). We would also like to thank the patients with tuberculosis who contributed to this study.

References

1 Chaves Torres NM, Quijano Rodríguez JJ, Porras Andrade PS, Arriaga MB, Netto EM. Factors predictive of the success of tuberculosis treatment: a systematic review with meta-analysis. *PLoS One* 2019; **14:** e0226507.

2 Urbanowski ME, Ordonez AA, Ruiz-Bedoya CA, Jain SK, Bishai WR. Cavitary tuberculosis: the gateway of disease transmission. *Lancet Infect Dis* 2020; **20:** e117–28.

3 Boehme CC, Nabeta P, Hillemann D, et al. Rapid molecular detection of tuberculosis and rifampin resistance. *N Eng J Med* 2010; **363:** 1005–15.

4 Hicks ND, Yang J, Zhang X, et al. Clinically prevalent mutations in *Mycobacterium tuberculosis* alter propionate metabolism and mediate multidrug tolerance. *Nat Microbiol* 2018; **3:** 1032–42.

5 Liu Q, Zhu J, Dulberger CL, et al. Tuberculosis treatment failure associated with evolution of antibiotic resilience. *Science* 2022; **378:** 1111–18.

6 Colangeli R, Jedrey H, Kim S, et al. Bacterial factors that predict relapse after tuberculosis therapy. *N Engl J Med* 2018; **379:** 823–33.

7 Holt KE, McAdam P, Thai PV, et al. Frequent transmission of the *Mycobacterium tuberculosis* Beijing lineage and positive selection for the EsxW Beijing variant in Vietnam. *Nat Genet* 2018; **50:** 849–56.

8 Thuong NT, Tram TT, Dinh TD, et al. MARCO variants are associated with phagocytosis, pulmonary tuberculosis susceptibility and Beijing lineage. *Genes Immun* 2016; **17:** 419–25.

9 Thai PV, Ha DT, Hanh NT, et al. Bacterial risk factors for treatment failure and relapse among patients with isoniazid resistant tuberculosis. *BMC Infect Dis* 2018; **18:** 1–9.

10 Saelens JW, Sweeney MI, Viswanathan G, et al. An ancestral mycobacterial effector promotes dissemination of infection. *Cell* 2022; **185:** 4507–25.

11 Flint J, Timpson N, Munafò M. Assessing the utility of intermediate phenotypes for genetic mapping of psychiatric disease. *Trends Neurosci* 2014; **37:** 733–41.

12 Jnawali HN, Ryoo S. First- and second-line drugs and drug resistance. In: Mahboub BH, Vats MG, eds. Tuberculosis - current issues in diagnosis and management. London: InTech, 2013.

13 Yang J, Pang Y, Zhang T, et al. Molecular characteristics and in vitro susceptibility to bedaquiline of *Mycobacterium tuberculosis* isolates circulating in Shaanxi, China. *Int J Infect Dis* 2020; **99:** 163–70.

14 Lu Y, Zheng M, Wang B, et al. Clofazimine analogs with efficacy against experimental tuberculosis and reduced potential for accumulation. *Antimicrob Agents Chemother* 2011; **55:** 5185–93.

15 Zhang F, Li S, Wen S, et al. Comparison of in vitro susceptibility of mycobacteria against PA-824 to identify key residues of Ddn, the deazoflavin-dependent nitroreductase from *Mycobacterium tuberculosis*. *Infect Drug Resist* 2020; **13:** 815–22.

16 Chang DP, Guan XL. Metabolic versatility of *Mycobacterium tuberculosis* during infection and dormancy. *Metabolites* 2021; **11:** 88.

17 Lees JA, Galardini M, Bentley SD, Weiser JN, Corander J. Pyseer: a comprehensive tool for microbial pangenome-wide association studies. *Bioinformatics* 2018; **34:** 4310–12.

18 Thomson M, Liu Y, Nunta K, et al. Expression of a novel mycobacterial phosphodiesterase successfully lowers cAMP levels resulting in reduced tolerance to cell wall-targeting antimicrobials. *J Biol Chem* 2022; **298:** 102151.

19 Snapper SB, Melton RE, Mustafa S, Kieser T, Jacobs WR Jr. Isolation and characterization of efficient plasmid transformation mutants of *Mycobacterium smegmatis*. *Mol Microbiol* 1990; **4:** 1911–19.

20 Jinich A, Zaveri A, DeJesus MA, et al. The *Mycobacterium tuberculosis* transposon sequencing database (MtbTnDB): a large-scale guide to genetic conditional essentiality. *bioRxiv* 2021; published online March 6. https://doi.org/10.1101/2021.03.05.434127

21 Sherman BT, Hao M, Qiu J, et al. DAVID: a web server for functional enrichment analysis and functional annotation of gene lists (2021 update). *Nucleic Acids Res* 2022; **50:** W216–21.

22 Coll F, McNerney R, Guerra-Assunção JA, et al. A robust SNP barcode for typing *Mycobacterium tuberculosis* complex strains. *Nat Commun* 2014; **5:** 4812.

23 WHO. Technical report on critical concentrations for drug susceptibility testing of medicines used in the treatment of drug-resistant tuberculosis. Geneva: World Health Organization, 2018.

24 Keren I, Minami S, Rubin E, Lewis K. Characterization and transcriptome analysis of *Mycobacterium tuberculosis* persisters. *mBio* 2011; **2:** 10–128.

25 Chang Y, Fox BG. Identification of Rv3230c as the NADPH oxidoreductase of a two-protein DesA3 acyl-CoA desaturase in *Mycobacterium tuberculosis* H37Rv. *Biochemistry* 2006; **45:** 13476–86.

26 Li S, Poulton NC, Chang JS, et al. CRISPRi chemical genetics and comparative genomics identify genes mediating drug potency in *Mycobacterium tuberculosis*. *Nat Microbiol* 2022; **7:** 766–79.

27 Rittershaus ES, Baek SH, Krieger IV, et al. A lysine acetyltransferase contributes to the metabolic adaptation to hypoxia in *Mycobacterium tuberculosis*. *Cell Chem Biol* 2018; **25:** 1495–505.

28 Smith CM, Baker RE, Proulx MK, et al. Host-pathogen genetic interactions underlie tuberculosis susceptibility in genetically diverse mice. *Elife* 2022; **11:** e74419.

29 Kadura S, King N, Nakhoul M, et al. Systematic review of mutations associated with resistance to the new and repurposed *Mycobacterium tuberculosis* drugs bedaquiline, clofazimine, linezolid, delamanid and pretomanid. *J Antimicrob Chemother* 2020; **75:** 2031–43.

30 Freschi L, Vargas R Jr, Husain A, et al. Population structure, biogeography and transmissibility of *Mycobacterium tuberculosis*. *Nat Commun* 2021; **12:** 6099.

31 Rustad TR, Sherrid AM, Minch KJ, Sherman DR. Hypoxia: a window into *Mycobacterium tuberculosis* latency. *Cell Microbiol* 2009; **11:** 1151–59.

32 Conradie F, Bagdasaryan TR, Borisov S, et al. Bedaquiline–pretomanid–linezolid regimens for drug-resistant tuberculosis. *N Engl J Med* 2022; **387:** 810–23.

33 Merker M, Kohl TA, Barilar I, et al. Phylogenetically informative mutations in genes implicated in antibiotic resistance in *Mycobacterium tuberculosis* complex. *Genome Med* 2020; **12:** 1–8.

34 Bateson A, Ortiz Canseco J, McHugh TD, et al. Ancient and recent differences in the intrinsic susceptibility of *Mycobacterium tuberculosis* complex to pretomanid. *J Antimicrob Chemother* 2022; **77:** 1685–93.

35 Stanley S, Liu Q, Fortune SM. *Mycobacterium tuberculosis* functional genetic diversity, altered drug sensitivity, and precision medicine. *Front Cell Infect Microbiol* 2022; **12:** 1478.